Elliptical Quantum Dots as On-Demand Single Photons Sources with Deterministic Polarization States

Chu-Hsiang Teng,[1] Lei Zhang,[2] Tyler A. Hill,[2] Brandon Demory,[1] Hui Deng,[2] and Pei-Cheng Ku[1]*

[1]*Department of Electrical Engineering and Computer Science, University of Michigan, 1301 Beal Ave., Ann Arbor, MI 48105, USA*

[2]*Department of Mechanical Engineering, University of Michigan, 2350 Hayward St., Ann Arbor, MI 48105, USA*

*peicheng@umich.edu

Abstract: In quantum information, control of the single photon's polarization is essential. Here we demonstrate single photon generation in a pre-programmed and deterministic polarization state, on a chip-scale platform, utilizing site-controlled elliptical QDs synthesized by a top-down approach. The polarization from the QD emission is found to be linear with a high degree of linear polarization and parallel to the long axis of the ellipse. Single photon emission with orthogonal polarizations is achieved, and the dependence of the degree of linear polarization on the QD geometry is analyzed.

On-demand single photon sources (SPS) play a key role in quantum science and technologies.[1] In quantum key distribution (QKD), single photons serve as the information carrier in which the secured information is directly encoded in the quantum state of photons represented by their polarizations. A QKD transmitter requires an SPS capable of generating photons in a single or multiple pre-defined linear polarization states.[2] In this study, we demonstrate elliptical quantum dot (QD) fabrication by a top-down process and show that an elliptical nitride semiconductor QD can generate single photons in a pre-defined quantum state determined by the orientation of the QD. A high degree of linear polarization (DLP) can be realized from these elliptical QDs via engineering of the hole wavefunctions. Furthermore, the top-down synthesis is simple, scalable, and offers a superior control of QD positions and emission wavelengths than more commonly-used bottom-up synthesis does

The polarization properties of semiconductor QD emission are determined by the symmetry of the electron and hole wavefunctions in the excitonic state. The symmetry of the hole wavefunction is sensitive to the strain distribution in the QD which depends on the QD shape, underlying substrate, and the strain field inside the QD. To generate a deterministic linear polarization state, one needs a hole wavefunction that is highly asymmetric with a high degree of directionality. This can be achieved with a strain field of similar asymmetry. Quantum dots have been fabricated at the tips of pyramidal structures that were pre-strained along a specific direction to control the photon polarization.[3] In this work, we propose to directly control the directionality of the strain field via the QD shape using a top-down approach on c-plane InGaN/GaN QDs. This has several advantages. First, the direction of the linear polarization can be arbitrary as it is not restricted by the underlying structures or substrates. Second, the electrical injection can be easily implemented due to the planar geometry. Third, the integration of QDs with other optical structures such as cavities is simpler without the underlying structures.

We chose to work on nitride semiconductor QDs. These QDs are ideally suited for on-demand SPS applications.

The exciton binding energy is large,[4] making room-temperature operation possible. The surface recombination velocity is small[5] and thus site-controlled QDs with etched interfaces can possess optical qualities comparable to that of self-assembled QDs.[6,7] Importantly, the energy spacings between heavy hole (HH), light hole (LH), and split-off (SO) bands in nitride semiconductors are small. As a result, a high DLP is expected from these QDs.[8-14]

Different top-down approaches have recently been reported to fabricate InGaN QDs,[6,15] aiming to improve the control of QD sizes, shapes, and positions. The elliptical QDs used in this work were synthesized by lithography and etching to enable a precise control of the QD shape including both the (in-plane) aspect ratio and orientation. Disk-shaped InGaN QDs with GaN barriers were formed by etching a single 3-nm thick InGaN/GaN quantum well (QW) as shown in Figure 1(a). Details of fabrication procedures are provided in the supplementary material.[16] Compared to binary GaN QDs, the use of InGaN alloys shifts the emission wavelength from ultraviolet to visible and improves the sensitivity of single photon detection using silicon based avalanche photodiodes. No indium clustering was found in the InGaN region as confirmed by the atom-probe tomography.[17] The optical properties of circular InGaN QDs fabricated by the same top-down approach have been studied before and reported elsewhere.[6,7]

The top-view scanning electron micrograph (SEM) of as-fabricated elliptical InGaN QDs embedded in GaN nanopillars is shown in Figure 1(b) for four different QD orientations, 45º apart. The dimensions of the InGaN QDs were inferred from the diameters at the top of the GaN nanopillars and the sidewall slanting angle as illustrated in Figure 1(a). Compared to QDs fabricated from the bottom-up approach, the top-down approach adopted in this work offered a much better control over the QD properties including positions and emission wavelengths. The lack of wetting layers for the top-down QDs can also reduce the background noise in single-photon emission.[3]

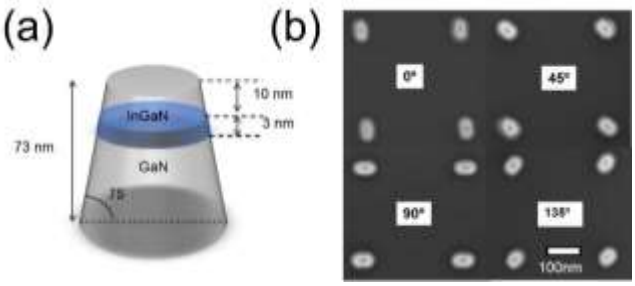

Figure 1. (Color online) (a) The schematic of the elliptical QD synthesized by a top-down process. The disk-shaped InGaN QD is sandwiched by GaN barrier materials. (b) The top-view scanning electron micrographs of four different QD orientations: 0º, 45º, 90º, and 135º.

The polarization properties of QD emission were measured by polarization-resolved micro-photoluminescence (μ-PL). A Hanbury Brown-Twiss interferometer was used to obtain the second-order autocorrelation function g(2) which confirmed whether or not the QD emitted single photons. The detailed description of μ-PL setup is described in the supplementary material,[16] and the numerical fitting model for $g^{(2)}$ can be found in Reference 6. All measurements were performed at 10 K to optimize the signal-to-noise ratio. Off-resonant optical excitation below the GaN bandgap at an intensity of 102 W/cm^2 was used. Figures 2(a) shows the polarization-resolved emission spectra at different linear polarizer angles for two QDs (QD A and QD B). QD A and QD B were designed to have orientations orthogonal to each other. The orientation of QD A was assigned as 0º which was not aligned to any particular crystal plane. The designed (nominal) dimensions of both QDs were 22 nm by 36 nm for their short and long axes, respectively with an (in-plane) aspect ratio of 1.64. The spectra revealed highly polarized exciton emission peaks at 2.979 and 2.958 eV for QD A and B respectively and optical-phonon peaks ~90 meV below the exciton peaks.[18] Only the exciton peaks were selected for polarization analysis. Figure 2(b) shows the polar plots of the normalized integrated PL intensities of the exciton peaks for both QDs. By fitting the measured polar plots, the polarization direction and DLP from the QD

emission can be determined. With a 95% confidence interval, the photon polarizations were determined to be -0.8° ± 1.9° and 98.7° ± 4.5° for QD A and QD B respectively; the DLP's were determined to be 0.905 ± 0.075 and 0.9 ± 0.1 for QD A and QD B, respectively. Photon antibunching was confirmed for both QDs as shown in Figure 2(c). While the measurement was done with pulsed laser excitation, the long carrier lifetime (Figure 2(d)) due to built-in polarization field lead to significant overlap between neighboring peaks in $g^{(2)}$ plots.[7] In addition, the bi-exciton emission peaks could not be well resolved and separated from exciton peaks given that the linewidth was comparable to the energy difference between exciton and bi-exciton.[19] The peak overlap and possible bi-exciton emission were included in the $g^{(2)}$ fitting model.[6] The fitting rendered $g^{(2)}(0) = 0.26$ for QD A and 0.32 for QD B without subtracting any background.

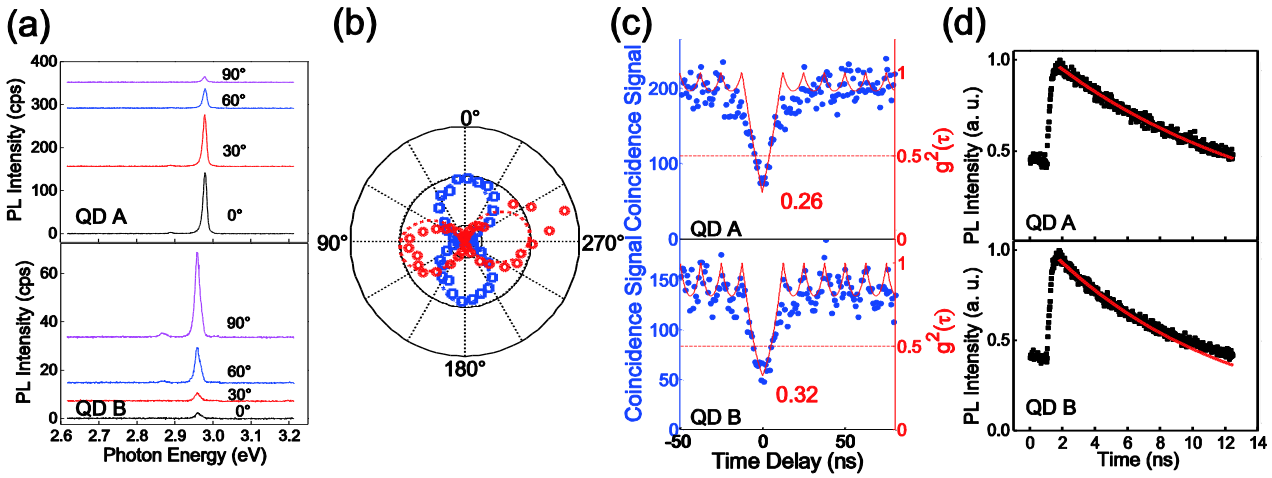

Figure 2. (Color online) (a) Polarized PL spectra from QD A and B at various polarization angles. (b) Polar plots of normalized PL intensity of QD A (blue) and B (red) and the corresponding fitting curves (dotted lines) using $I_{min}+(I_{max}-I_{min})\cos^2(\theta-\theta_{ref})$ where θ_{ref} was the fitted polarization angle. The degree of linear polarization (DLP) was calculated based on $(I_{max}-I_{min})/(I_{max}+I_{min})$ from the fitting curves. (c) $g^{(2)}(\tau)$ of QD A and B subjected to 102 W/cm^2 of excitation intensity. (d) Time-resolved PL and exponential fitting (red curves). The $g^{(2)}$ fitting rendered lifetime values 13.7 ± 3.45 ns and 9.3 ± 1.25 ns for QD A and B respectively, and the fitting of time-resolved PL resulted in 14.6 ± 0.46 ns and 11.1

± 0.42 ns lifetime. The deviation of QD B from a single exponential fitting after 8 ns is attributed to the background emission from the substrate.

Figure 3(a) and (b) summarize the polarization angles and DLP's measured from a total of 60 QDs randomly selected from five different QD orientations. The results showed a good correlation between the polarization angle and the QD orientation. Although all QDs had the same nominal dimensions (22nm by 36nm) and aspect ratio (1.64), the measured polarization angle for a given QD (nominal) orientation exhibits a standard deviation of 13º. The measured DLP has an average of 0.72 and a standard deviation of 0.17. To investigate the origin of these variations, we analyzed the shapes of 80 QDs using SEM. The 80 QDs were designed to have the same nominal lateral aspect ratio, 1.64, but ended up having slightly different geometry because of process variations. It was found that the QD orientation and the aspect ratio exhibited a standard deviation of 6° and 0.25 respectively. The 0.25 variation in the aspect ratio corresponds to 0.16 standard deviation in DLP according to Figure 5. These variations were limited by the e-beam lithography process we used. The other possible source of variations is the local indium fluctuation originated from the random nature of ternary alloy but can potentially be eliminated by using GaN QDs.[20]

The QD shapes were also not all elliptical. A small number of QDs exhibited shapes significantly deviated from elliptical shapes. Figure 4 shows a few examples of these "deformed" QDs and their corresponding polar plots. Figure 4(a) shows a QD exhibiting a near circular shape and a DLP of only 0.35. Figure 4(b) shows a QD exhibiting an aspect ratio larger than designed and therefore a much higher DLP of 0.98. Figure 4(c) shows a QD with an orientation -13º deviated from the design and the measured polarization angle was -20.7º.

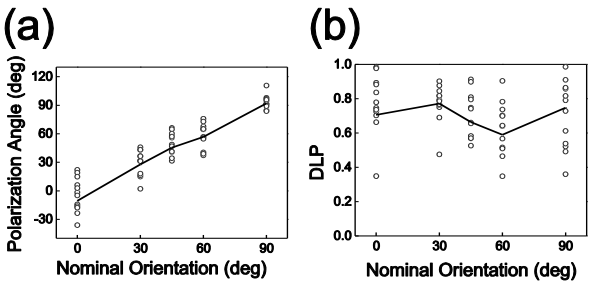

Figure 3. (a) Measured polarization angle and (b) DLP as a function of the designed QD orientation angle. The data points represent measurement results of twelve individual QDs that were randomly selected at each QD orientation angle, and the solid curves correspond to the median values of the polarization angles and DLPs.

Another observation made from Figure 3 was that there was not a single QD orientation which showed a significantly higher DLP. This is also true from a different set of data obtained from another sample. Given that the orientations of elliptical QDs were not intentionally aligned to any crystal plane, the similar DLP values for different orientations suggested that the polarization properties were not sensitive to the underlying crystal symmetry. If it were the case, QDs oriented along 45º and 135º would express slightly different properties than QDs oriented along 30º and 60º due to the six-fold symmetry of the c-plane wurtzite lattice on which the InGaN QW was grown. Furthermore, the measured photon energies for different QD orientations were 2.979 ± 0.024, 2.968 ± 0.019, 2.971 ± 0.015, 2.971 ± 0.044, 2.968 ± 0.033 eV for 0º, 30º, 45º, 60º, 90º, respectively. The spectral linewidths were 17 ± 5, 22 ± 8, 18 ± 6, 19 ± 6, 21 ± 7 meV for 0º, 30º, 45º, 60º, 90º, respectively. There was no systematic dependence of the spectral properties of QDs on their orientations either. Besides, we have not observed any obvious dependence of DLP on the excitation intensity up to 250 W/cm^2. Thus we conclude that the polarization properties of elliptical c-plane InGaN QDs are determined geometrically by the QD shape. As suggested by the six-fold symmetric wurtzite structure, similar degrees of polarization were found regardless of the polarization angle. As a result, one may expect to generate any

polarization angle with a high DLP from these QDs on a single chip, and the top-down approach is a viable approach in controlling both QD geometry and polarization.

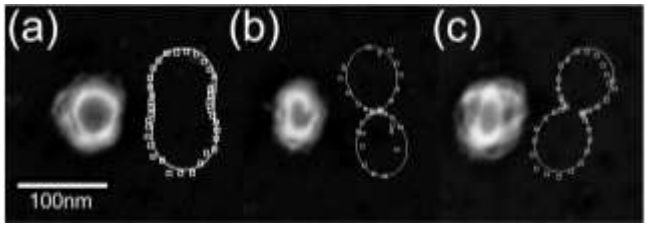

Figure 4. The top-view SEM images and the polar plots of the polarization properties of three QDs exhibiting irregular orientations or/and shapes compared to the designed parameters. The SEM images are more blurry compared to those shown in Figure 2(b) because the chromium etch masks have been removed before imaging was performed in this figure in order to reveal the true shape of the top surface of the nanopillar. (a) shows a QD whose shape has become almost circular and (b) and (c) show two QDs with aspect ratio and orientation deviated from design, respectively.

Last, using the actual QD in-plane aspect ratios measured by SEM, we plotted the measured DLP versus the QD aspect ratio in Figure 5 together with calculated results based on the 6-band k·p model which took into account the effect of strain.[16,17,21] The seven QDs were from the same array, having the same nominal lateral aspect ratio of 1.64, but ended up with different geometry because of process variation. The measured DLP values agreed qualitatively with theoretical values. Calculations were also performed for other QD materials. A DLP approaching unity is possible with a nitride QD aspect ratio close to 2. It was also observed that nitride QDs exhibit much higher DLP's compared to other common III-V or II-VI materials. This is consistent with the hypothesis that a stronger valence band mixing is key to a higher DLP in nitride semiconductors due to the small split-off energy.[9,22-25]

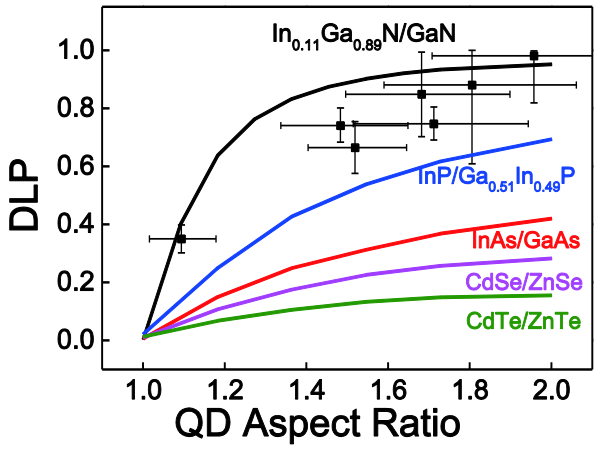

Figure 5. The calculated degree of linear polarization (DLP) of elliptical QDs for a variety of different semiconductors as a function of QD in-plane aspect ratio. The short axis is fixed at a constant 22 nm which is the same as the short axis length of QDs used in experiments in this work. The QD and barrier materials are given in the graph. The discrete data points correspond to the experimental data obtained from this study. The vertical error bars represent the DLP fitting errors, and the horizontal error bards are the SEM measurement uncertainty, which was ±1.5 nm.

In summary, site-controlled elliptical InGaN QDs were fabricated and polarized single photon emission was observed. The polarized emission is solely controlled by the orientation of the QD and is insensitive to the underlying crystal symmetry. The DLP is high and can approach unity when the QD lateral aspect ratio is close to two. Good correlations between the QD geometry and the polarization properties were found. Deviation of the polarization direction from the nominal QD orientation has been largely attributed to patterning errors originating from lithography and etching. The top-down approach offered an unprecedented degree of control over the QD position and emission wavelength not easily attainable from a bottom-up approach. Because the polarization control is an intrinsic property of the elliptical QD without the assistance of any external structures, multiple QDs of different polarizations can be placed in close proximity. Electrically driven single photon devices could also be readily made with proper planarization and metal contacts.[26] It allows each QD to be individually addressable, enables the control of output

polarization, and can be convenient for quantum cryptography applications.

This work was supported by the National Science Foundation under Awards DMR 1409529 (for fabrication and measurements) and DMR 1120923 (for theory). Part of the fabrication was performed in the Lurie Nanofabrication Facility which was part of the NSF NNIN network.

References

[1]C. Santori, D. Fattal, and Y. Yamamoto, *Single-photon devices and applications* (John Wiley & Sons, 2010).

[2]C. H. Bennett and G. Brassard, *Proceedings of IEEE International Conference on Computers, Systems and Signal Processing, Bangalore* (1984), p. 175.

[3]A. Lundskog, C. W. Hsu, K. F. Karlsson, S. Amloy, D. Nilsson, U. Forsberg, P. O. Holtz, and E. Janzén, Light: Science & Applications **3**, e139 (2014).

[4]B. Monemar, Physical Review B **10**, 676 (1974).

[5]J. B. Schlager, K. A. Bertness, P. T. Blanchard, L. H. Robins, A. Roshko, and N. A. Sanford, Journal of Applied Physics **103**, 124309 (2008).

[6]L. Zhang, C.-H. Teng, T. A. Hill, L.-K. Lee, P.-C. Ku, and H. Deng, Applied Physics Letters **103**, 192114 (2013).

[7]L. Zhang, T. A. Hill, C.-H. Teng, B. Demory, P.-C. Ku, H. Deng, Physical Review B **90**, 245311 (2014).

[8]M. Winkelnkemper, R. Seguin, S. Rodt, A. Schliwa, L. Reissmann, A. Strittmatter, A. Hoffmannm, and D. Bimberg, Journal of Applied Physics **101**, 113708 (2007).

[9]R. Bardoux, T. Guillet, B. Gil, P. Lefebvre, T. Bretagnon, T. Taliercio, S. Rousset, and F. Semond, Physical Review B **77**, 235315 (2008).

[10]M. Winkelnkemper, R. Seguin, S. Rodt, A. Hoffmann, and D. Bimberg, Journal of Physics: Condensed Matter **20**, 454211 (2008).

[11]C. Kindel, S. Kako, T. Kawano, H. Oishi, Y. Arakawa, G. Hönig, M. Winkelnkemper, A. Schliwa, A. Hoffmann, and D. Bimberg, Physical Review B **81**, 241309 (2010).

[12]S. Amloy, Y. T. Chen, K. F. Karlsson, K. H. Chen, H. C. Hsu, C. L. Hsiao, L. C. Chen, and P. O. Holtz, Physical Review B **83**, 201307 (2011).

[13]S. Amloy, K. F. Karlsson, T. G. Andersson, and P. O. Holtz, Applied Physics Letters **100**, 021901 (2012).

[14]S. Kremling, C. Tessarek, H. Dartsch, S. Figge, S. Höfling, L. Worschech, C. Kruse, D. Hommel, and A. Forchel, Applied Physics Letter **100**, 061115 (2012).

[15]X. Xiao, A. J. Fischer, G. T. Wang, P. Lu, D. D. Koleske, M. E. Coltrin, J. B. Wright, S. Liu, I. Brener, G. Subramania, and J. Y. Tsao, Nano Letters **14**, 5616 (2014).

[16]See supplementary material at [URL will be inserted by AIP] for details of sample fabrication, photoluminescence measurements, and numerical simulation of degree of linear polarization.

[17]C.-H. Teng, L. Zhang, L. Yan, J. Millunchick, H. Deng, and P.-C. Ku, presented at International Symposium of Compound Semiconductor (2014).

[18]S. J. Lee, J. O. Kim, S. K. Noh, K. S. Lee, Journal of Korean Physics Society **51**, 1027 (2007).

[19]S. Amloy, K. F. Karlsson1, M. O. Eriksson1, J. Palisaitis1, P. O. Å. Persson, Y. T. Chen, K. H. Chen, H. C. Hsu, C. L. Hsiao, L. C. Chen, and P. O. Holtz, Nanotechnology **25**, 495702 (2014).

[20] S. Schulz, M. A. Caro, C. Coughlan, and E. P. O'Reilly. Physical Review B **91**, 035439 (2015)

[21]S. L. Chuang, C. S. Chang, Physical Review B **54**, 2491 (1996).

[22]I. Vurgaftman and J. R. Meyer, Journal of Applied Physics **94**, 3675 (2003).

[23]I. Vurgaftman, J. R. Meyer, and L. R. Ram-Mohan, Journal of Applied Physics **89**, 5815 (2001).

[24]W. Shan, J. J. Song, H. Luo, and J. K. Furdyna, Physical Review B **50**, 8012 (1994).

[25]J. Piprek, *Semiconductor optoelectronic devices: Introduction to physics and simulation* (Academic Press, 2003).

[26]L. Zhang, C.-H. Teng, P.-C. Ku, H. Deng, presented at CLEO: QELS_Fundamental Science, Optical Society of America (2014).

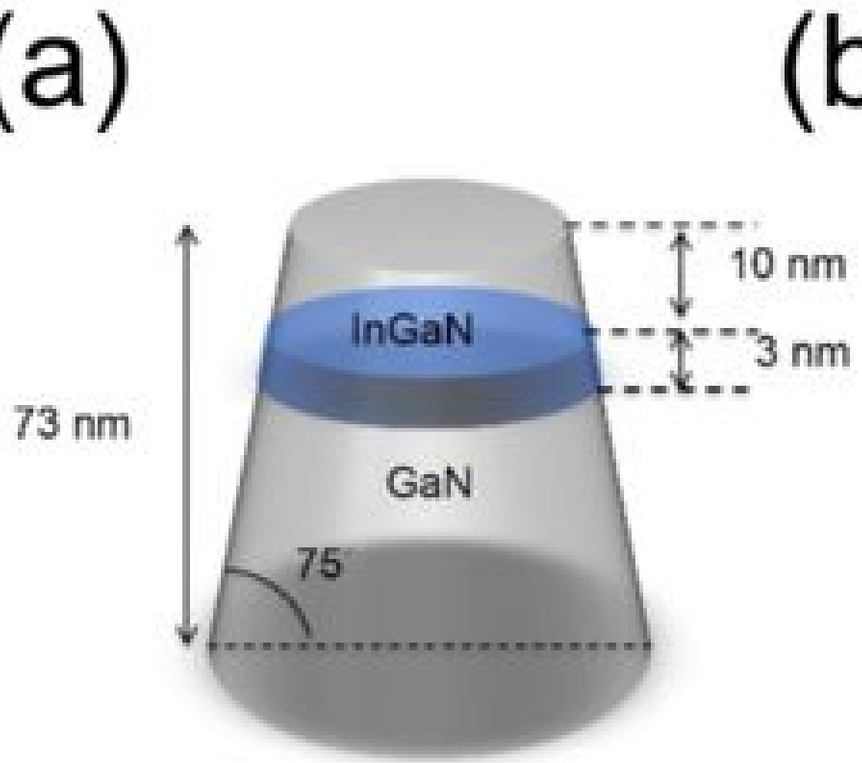

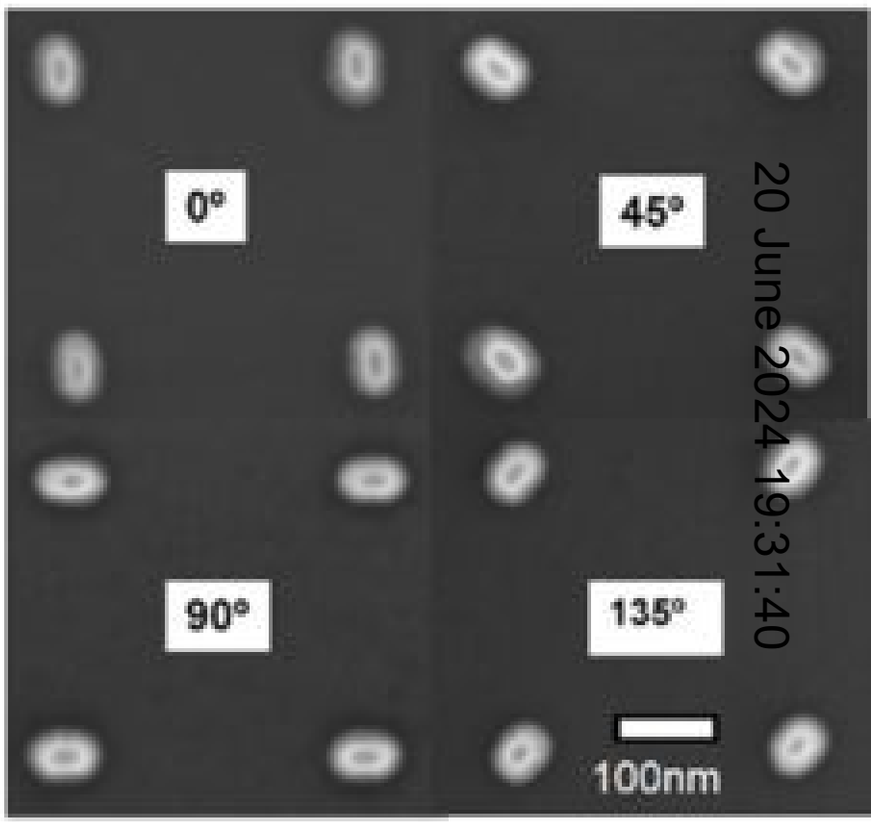

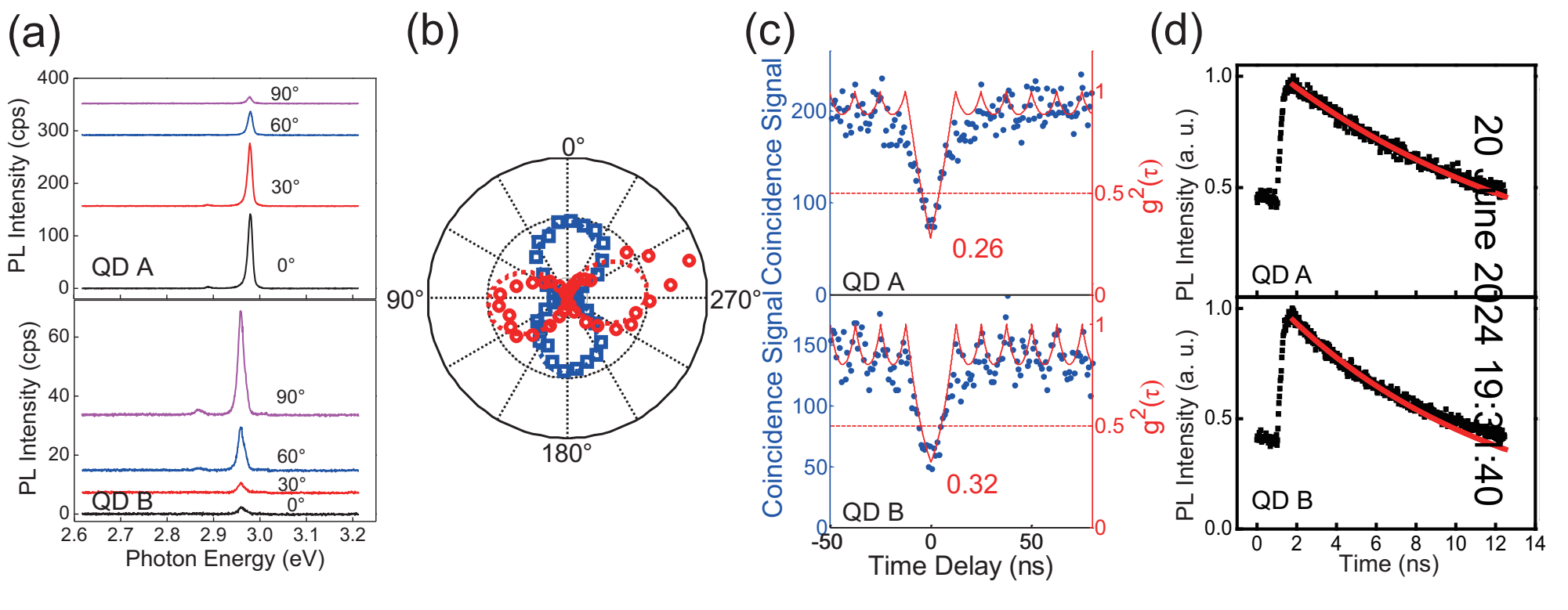
(a)
PL Intensity (cps)
QD A
90°
60°
30°
0°
QD B
Photon Energy (eV)
(b)
0°
90°
180°
270°
(c)
Coincidence Signal
$g^2(\tau)$
0.26
0.32
QD A
QD B
Time Delay (ns)
(d)
PL Intensity (a. u.)
QD A
QD B
Time (ns)
20 June 2024 19:31:40

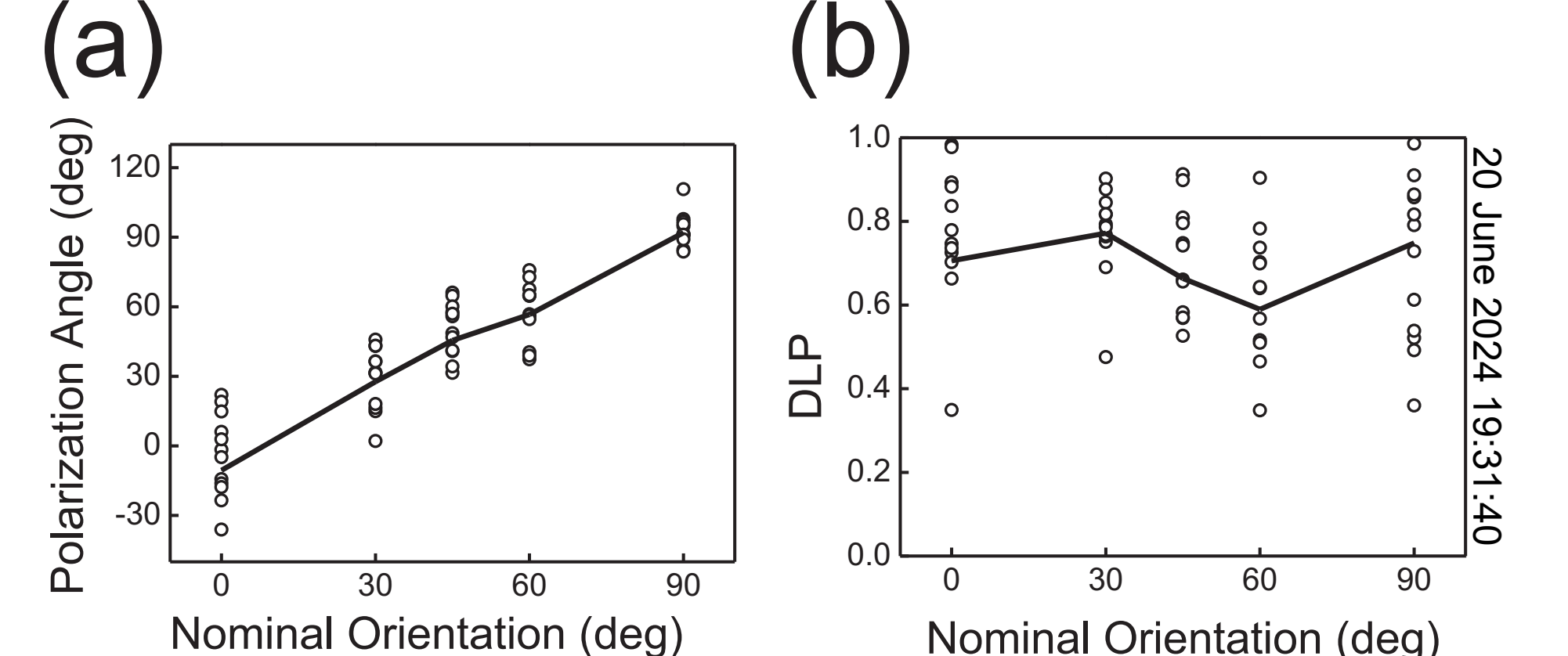
(a)
Polarization Angle (deg)
120
90
60
30
0
-30
0
30
60
90
Nominal Orientation (deg)
(b)
DLP
1.0
0.8
0.6
0.4
0.2
0.0
0
30
60
90
Nominal Orientation (deg)
20 June 2024 19:31:40

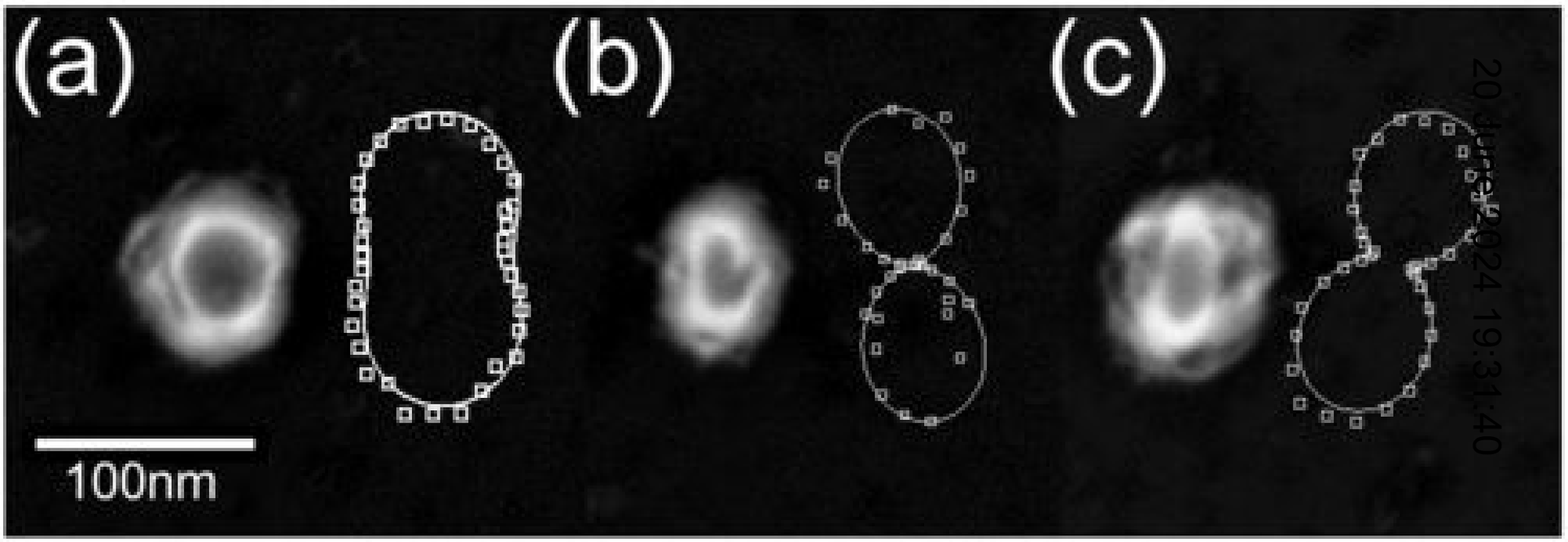
(a)
(b)
(c)
100nm

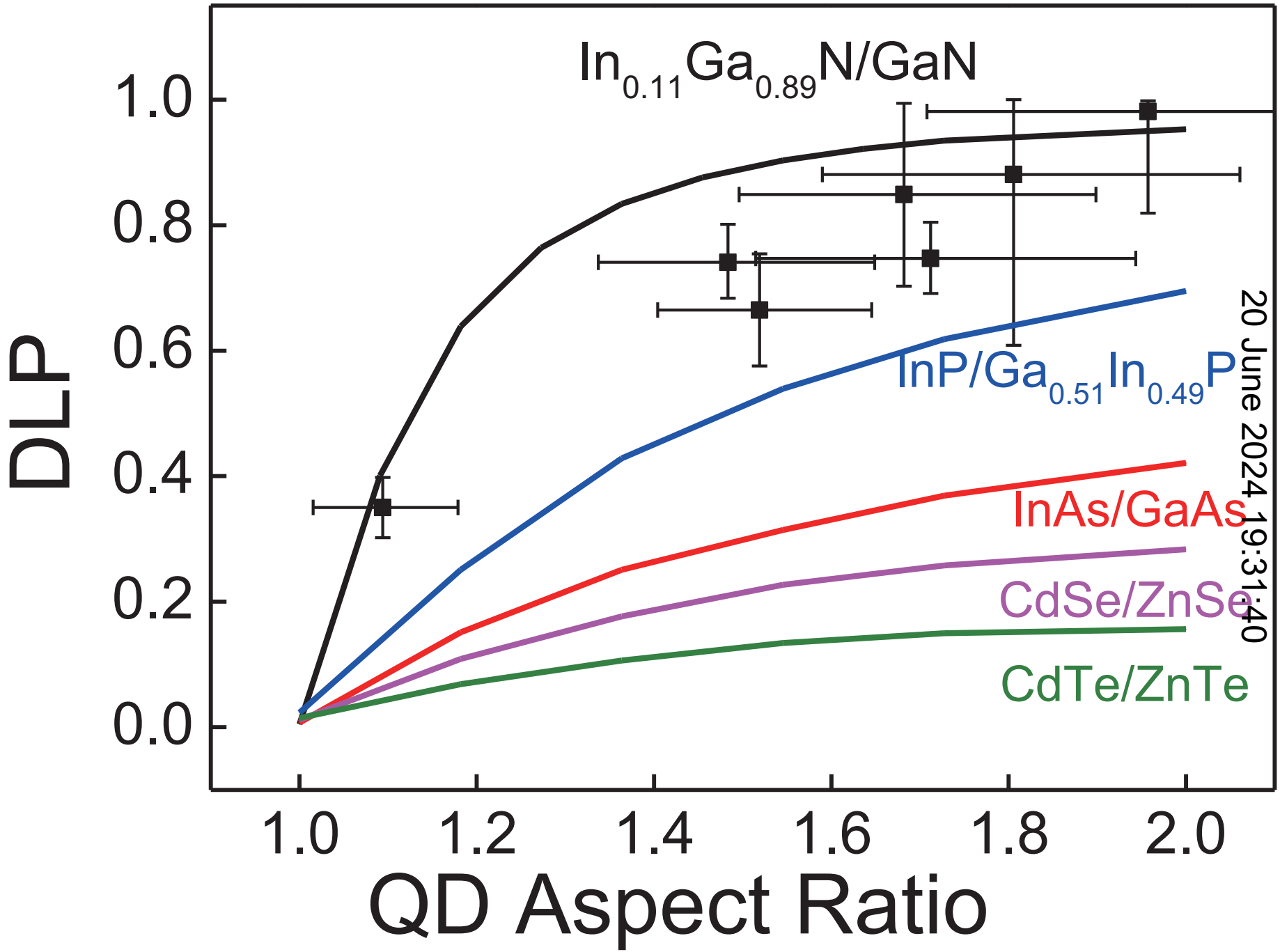
In0.11Ga0.89N/GaN
InP/Ga0.51In0.49P
InAs/GaAs
CdSe/ZnSe
CdTe/ZnTe
DLP
QD Aspect Ratio
1.0
0.8
0.6
0.4
0.2
0.0
1.0
1.2
1.4
1.6
1.8
2.0
20 June 2024 19:31:40